Climente Alarcon, V.; J. Antonino-Daviu; Riera-Guasp, M.; Pons Llinares, J.; José Roger-Folch; Jover-Rodriguez, P.; Arkkio, A. (2011). Transient tracking of low and high-order eccentricity-related components in induction motors via TFD tools. Mechanical Systems and Signal Processing. 25(2):667-679. doi:10.1016/j.ymssp.2010.08.008

Transient tracking of low and high-order eccentricity-related components in induction motors via TFD tools

V. Climente-Alarcón* , J. Antonino-Daviu * P. Jover-Rodriguez** A. Arkkio***

M. Riera-Guasp * , J. Pons-Llinares *,

J. Roger-Folch*

* Universidad Politécnica de Valencia
Departamento de Ingeniería Eléctrica
P.O.Box 22012, 46071 Valencia, SPAIN
Phone: 0034-96-3877592,
Fax: 0034-96-3877599
e-mail: joanda@die.upv.es

** ABB Corporate Research
Forskargränd 8
72222 Vasteras, SWEDEN
Phone: 0046-730757030
e-mail: pedro.rodriguez@se.abb.com

*** Department of Electrical Engineering
Aalto University
P.O. Box 13000, FI-00076, FINLAND
Phone: +358-9-4512991,
Fax: +358-9-4512392
e-mail: antero.arkkio@tkk.fi

Abstract: The present work is focused on the diagnosis of mixed eccentricity faults in induction motors via the study of currents demanded by the machine. Unlike traditional methods, based on the analysis of stationary currents (*Motor Current Signature Analysis*, *MCSA*), this work provides new findings regarding the diagnosis approach proposed by the authors in recent years, which is mainly focused on the fault diagnosis based on the analysis of transient quantities, such as startup or plug stopping currents (*Transient Motor Current Signature Analysis*, *TMCSA*), by using suitable Time-Frequency Decomposition (TFD) tools. The main novelty of this work is to prove the usefulness of tracking the transient evolution of high-order eccentricity-related harmonics in order to diagnose the condition of the machine, complementing the information obtained with the low-order components, whose transient evolution was well characterised in previous works. Tracking of high-order

eccentricity-related harmonics during the transient, through their associated patterns in the time-frequency plane, may significantly increase the reliability of the diagnosis, since the set of fault-related patterns arising after application of the corresponding TFD tool, is very unlikely to be caused by other fault or phenomena. Although there are different TFD tools which could be suitable for the transient extraction of these harmonics, this paper makes use of a Wigner-Ville Distribution (WVD)-based algorithm in order to carry out the time-frequency decomposition of the startup current signal, since this is a tool showing an excellent trade-off between frequency resolution at both high and low frequencies. Several simulation results obtained with a Finite Element-based model as well as experimental results show the validity of this fault diagnosis approach under several faulty and operating conditions. Also, additional signals corresponding to the coexistence of the eccentricity and other non-fault related phenomena making difficult the diagnosis (fluctuating load torque) are included in the paper. Finally, a comparison with an alternative TFD tool - the Discrete Wavelet Transform (DWT) - applied in previous papers, is also carried out in the contribution. The results are promising regarding the usefulness of the methodology for the reliable diagnosis of eccentricities and for their discrimination against other phenomena.

1. INTRODUCTION

Eccentricities are caused by non-uniform air-gap between stator and rotor [1]. They are rather common faults in AC electrical machines and, specifically, in induction motors, which constitute the most spread electrical machines in the industrial environment [2]. According to some surveys, mechanical faults amount for 50% to 60% of the faults taking place in electric motors. Around 60% of the mechanical failures taking place in this type of machines are related to eccentricities [3]. Indeed,

eccentricities are often directly derived from other faults occurring in the machine such as bearing failures or misalignments. Besides, other external phenomena such as load torque oscillations may lead to mechanical stresses increasing the severity of the aforementioned failure. The consequences of this fault can be severe; it might even lead to a collapse of the machine due to rotor-to-stator rub [4-5].

The two most important types of eccentricity are; the *static eccentricity* and the *dynamic eccentricity* [1]. In the case of the *static eccentricity*, the position of minimum air-gap remains fixed in space. This type of eccentricity can be due to reasons such as ovality of the rotor or to an incorrect placement of the rotor or stator, which can be caused by incorrect support of the bearings, bearing deterioration, deformation of the housings, excessive tolerance, etc…[1,6-7] . Fig. 1 shows these two possible ways for occurrence of static eccentricity; in Fig. 1 (a), the eccentricity is caused by incorrect placement, so that the rotor rotates around its geometric centre, but this does not coincide with the stator centre. Fig. 1 (b) shows a static eccentricity due to ovality of the stator.

On the other hand, in the case of *dynamic eccentricity*, the position of minimum air-gap does not remain fixed in space, but it rotates together with the rotor. This eccentricity can be due to an ovality of the rotor (Fig. 2 (b)) or to the fact that the rotor rotates around the stator centre, which does not coincide with the geometric centre of the rotor (Fig. 2 (a)) [6]. Dynamic eccentricity can be due to reasons such as deformation of the rotor shaft, bearing wear or misalignment or mechanical resonance at critical speed [1].

The combination between static and dynamic eccentricity is known as *mixed eccentricity*, which is the most usual situation in practice; in this case, the rotation axis of the rotor coincides neither with its geometric centre nor with the stator centre. A possible case of mixed eccentricity is shown in Fig. 3.

The classical method for diagnosis of eccentricities, as well as other electromechanical faults, in the industrial environment has been mainly based on the analysis of the current demanded by the machine during steady-state operation and the further application of suitable tools for stationary signals analysis,

such as the Fast Fourier Transform (FFT). This methodology, though robust, has some important drawbacks in certain situations, which may be rather common in the industrial environment [8-9].

For instance, in case of eccentricity diagnosis, it has been proven that when the machine operates under pulsating load torques (situation quite common when driving compressors, pumps or other mechanisms involving gear reducers), some components appear in the FFT spectrum. These components may be quite similar to those introduced by the eccentricity fault, thus leading to confusion or even to a wrong diagnosis of the fault [4-5]. This problem is often aggravated by the fact that eccentricity-related components usually ~~often~~ have very low amplitudes, unless the level of failure in the machine is severe enough, a fact that makes their detection sometimes difficult. On the other hand, other faults (such as bearing failures or even broken bars) could also introduce frequency components which may be confused with those created by eccentricities, mainly in the high-frequency region.

These and other reasons have led to propose the study of the current demanded by the machine during the transient processes through which it operates, as a supplementary approach to complement the diagnostic information obtained from stationary analysis [4-5, 9-14]. Specifically, the authors of this paper proposed, in recent works, the study and analysis of transient currents, such as the startup current or the current demanded by the machine during a plug stopping [14]. The idea underlying this methodology is to trace the time-frequency evolutions of characteristic fault-related components during the transient regime under study. These evolutions lead to very particular patterns in the time-frequency plane, which can be used for the diagnosis of the corresponding faults. The pattern created by a component related to a specific fault is very unlikely to be caused by another component related to other fault or phenomena; this fact substantially increases the reliability of the methodology. Besides, the detection of a time-frequency evolution provides much more information than detecting a single peak in the FFT spectrum, which is more likely to be masked by other phenomena.

The proposed transient-based approach was successfully applied in previous works to the detection of broken rotor bars [9, 14-15], eccentricities [4-5] or even stator short-circuits [5]. It is important to remark that the aim of the proposed methodology is not to substitute the classical steady-state FFT method in those applications in which it works well (i.e. pure stationary conditions), but to complement it in those cases in which its application may not be appropriate or could lead to a wrong diagnostic conclusion.

Despite the notable advances in this area, most of the developed works have been focused on tracing the low-order harmonics introduced by the fault (sideband components in the case of rotor bar breakages, low-frequency harmonics in the case of eccentricities). Few works have dealt with the transient extraction of high-order fault-related harmonics during the startup or other transient [16-17]. The use of these high-frequency fault-related components may provide important information for fault diagnosis purposes, as defended by some authors for steady-state analysis [6]. For instance, load torque fluctuations often have a more significant influence on the low-frequency region, rather than on the high-frequencies. This is due to the fact that it is less likely to have load pulsations capable to modulate the current at so high frequencies, mainly when the inertia of the group motor-load is high [6]. Therefore, the fault-related components evolving in the high-frequency region should be less 'polluted' due to the presence of this phenomenon. Furthermore, in the case of other faults such as rotor asymmetries, effects such as inter-bar currents have a greater influence on the low-frequency fault-related components than on the high-order ones [6].

Therefore, tracking the evolution of the high-frequency eccentricity-related components may provide very interesting information to diagnose the condition of the machine, complementing that information provided by the detection of low-order fault-related harmonics. In any case, it should be remarked that the detection of these high-frequency components is not always easy, due to the fact that they have

often much lower amplitudes that the main eccentricity-related components located in the low-frequency region.

The main novelty of this paper is to characterize the theoretical evolution of high-order eccentricity-related components during the startup transient as well as to prove (both through simulations and experimental tests) their validity for diagnosing the condition of the machine, especially in cases in which the diagnostic reached according to the low-order harmonics might be not enough conclusive, e.g., under the presence of load torque oscillations.

Despite different TFD tools are valid for the objectives pursued, in this paper, Wigner-Ville Distribution (WVD) is applied in order to track the evolution of the eccentricity-related components evolving, both within the low and within the high frequency region, along the startup transient. In comparison with other TFD tools previously used in the literature for transient-based fault diagnosis (Discrete Wavelet Transform [4-5, 10-15], Continuous Wavelet Transform [18-20], Wavelet packets [21], Hilbert-Huang Transforms [22-24], Hilbert Transforms [25], etc…), WVD shows a good trade-off between computational requirements and frequency resolution both in the high and low frequency region. This latter property makes it suitable for the simultaneous extraction of high and low frequency fault-related components. However, the main drawback of the WVD is the possible appearance of cross-terms, this is, artifacts caused by the auto-correlation process carried out by this transform, which might mask the evolution of some relevant components in the time-frequency plane. Alternative improvements such as Choi-Williams Distributions (CWD) have been proposed to overcome this problem, though increasing the computational time required. A qualitative comparison between the WVD and an alternative tool, the DWT, is included in the paper; it reveals their corresponding advantages and drawbacks regarding the diagnosis of the considered fault, while demonstrating the validity of different TFD tools for the transient extraction of eccentricity-related components.

The results altogether prove the usefulness of the proposed approach and the potential of the tool for being used as a basis for the possible implementation of automatic fault diagnosis systems based on this philosophy.

2. ECCENTRICITY-RELATED COMPONENTS DURING THE STARTUP

Well-known expressions for the computation of the frequencies related to static and dynamic eccentricities are available in the literature [1, 7, 26]. If mixed eccentricities are present in the machine, components given by expression (1) or, equivalently, by (2) appear, where f is the supply frequency, f_r is the rotational frequency, p is the number of pole pairs and s is the slip ($s=\frac{n_s-n}{n_s}$, with n_s=synchronous speed and n= speed of the machine)[1, 7, 26].

$$f_{ecc} = f \pm k \cdot f_r \qquad \mathrm{k} = 1,2,3... \tag{1}$$

$$f_{ecc} = f \cdot \left[\left(1 \pm m \cdot \left(\frac{1-s}{p} \right) \right) \right] \quad , \quad m = 1,2,3... \tag{2}$$

As it can be observed, (2) depends on the slip s. Since this is a quantity varying from 1 to almost 0 during a direct startup (machine started being directly supplied from the mains), the components associated with the eccentricity will evolve in a very characteristic way during that transient. The most relevant components used for mixed eccentricity diagnosis are those obtained for m=1 in (2); the frequency of the first component (let us call it EC-25) for a two pole pair machine (p=2) will start being equal to the supply frequency f (=50 Hz in our case) when the machine is connected (s=1) and it will decrease, reaching almost $f/2$ (=25 Hz) when the steady-state is reached ($s\approx0$). The second component (EC-75) will have an initial frequency equal to f (s=1) evolving towards $3 \cdot f/2$ (=75 Hz)

($s \approx 0$). Tracking of these 'low-frequency' components during the startup has been proven to be a reliable way for the detection of eccentricities [4-5].

Additional eccentricity-related components can be obtained for higher values of m in (2). These higher-order components will also evolve in a particular manner during a direct startup as the slip s decreases from 1 to near 0. Table I shows the theoretical initial and final frequency values for the set of eccentricity-related components obtained for the initial values of m (from m=1 to m=5), for the case of a direct startup of a 2-pole pair machine with an steady-state slip of 0.001 (similar conditions to the induction machine which will be later simulated and tested).

The aim of this paper is to track the evolution of relevant components characterized in Table I during the transient, as a basis for the diagnostic of the machine condition. For this purpose, an improved Wigner-Ville Distribution-based method is applied to tested and simulated startup currents, taking advantage of the ability of this distribution for the simultaneous time-frequency analysis of high and low frequencies with enough frequency resolution. Viability of an alternative TFD tool for the same purpose is analyzed in section 5.

Table I. Eccentricity components according to (2) for p=2 and f=50 Hz: initial and final frequency values during the startup (in Hz)

Component	**m**	**Sign in (2)**	**Initial frequency value (connection, s=1)**	**Final frequency value (steady-state, s=0.001)**
EC-25	1	-	50	25.025
EC-75	1	+	50	74.975
EC-0	2	-	50	0.05
EC-100	2	+	50	99.95
EC-25-2	3	-	50	24.925

EC-125	3	+	50	124.93
EC-50	4	-	50	49.9
EC-150	4	+	50	149.9
EC-75-2	5	-	50	74.875
EC-175	5	+	50	174.875

3. IMPROVED WIGNER-VILLE DISTRIBUTION (WVD)-BASED METHOD

Foundations of WVD can be found in well-known available references [27]. The aim of this section is to provide a brief summary of the bases of this transform and to explain how its application has been adapted to the problem of interest.

WVD is a particular case of the Cohen class distributions which yields a time-frequency energy density computed by correlating the signal with a time and frequency translation of itself. The WVD of a signal *x(t)* is defined by (3):

$$W_X(t,\omega) = \frac{1}{2\pi}\int_{-\infty}^{+\infty} x\left(t+\frac{\tau}{2}\right)\cdot x^*\left(t-\frac{\tau}{2}\right)\cdot e^{-j\tau\omega}d\tau \tag{3}$$

where *x** denotes the conjugate of *x*. Thus, the Wigner integral is the Fourier transform, with respect to the delay variable τ, of $x(t+\tau/2)\ x^*(t-\tau/2)$. This procedure avoids any loss of time-frequency resolution, as it happens, for instance, when performing the windowing in the Short Time Fourier Transform [14].

In discrete form, the WV distribution is defined by (4) [28]:

$$WVD(n,k) = \sum_{p=-N}^{N-1} R[n,q]\cdot e^{-\frac{j2\pi kq}{N}} \tag{4}$$

where *R[n,q]* is the instantaneous correlation given by (5), *n* is the number of samples of the analytical or interpolated form of the discrete signal *x[n]* and *q* is an odd integer.

$$R[n,q] = x\left[n + \frac{q}{2}\right] \cdot x^*\left[n - \frac{q}{2}\right] \quad (5)$$

Despite the Wigner-Ville distribution is faster than other exponential algorithms and it has an excellent joint time-frequency resolution [28], its use is hindered by the appearance of outer interferences, when applied to the analysis of multicomponent signals. These interferences or artifacts, also known as *cross terms*, appear in the distribution at time instants or frequencies in which there should be no energy. As a consequence, it is advisable to calculate the WVD on the analytic signal obtained from the Hilbert transform [29] of the real signal, since the Fourier transform of an analytic signal has no negative frequency components and thus, there cannot be any interference between positive and negative frequency ones.

In order to further minimize the cross term problem, now appearing between the positive frequency components, authors added in the computation of the Time-Frequency distribution a two dimensional function called *kernel*, which originates new transforms with different features, such as the *Choi-Williams distribution*.

As these modifications come at the expense of adding some limitations in other desirable properties, the general procedure nowadays consists of selecting the kernel accordingly to the duty to be developed, that is, selecting among all the Cohen class distributions, the best fitted for each task.

Instead of that, the WVD-based algorithm used in this paper is based on ~~proposes~~ an alternative way to minimize the drawback caused by the cross-terms; here, it has been preferred to keep the higher resolution of the WVD, -that is, choosing the Kernel equal to "1"– since lower amplitude harmonics are to be detected. Cross terms are either tolerated or minimized by filtering the signal prior to the analysis, in order to eliminate the constant frequency components (e.g. fundamental supply frequency) and keep only the frequency bands in which the fault effects are present.

This filtering procedure is applied gradually, eliminating the supply frequency component in all

cases and removing higher order constant frequency ones as needed. Chebyshev and Elliptic filters, as implemented in MATLAB and shown in Appendix A, are suitable for this task.

When the study is focused on a specific time-frequency box, the signal is also filtered by means of high and low pass Butterworth filters fitted to the limit frequencies. Further, down sampling eases the computational requirements**.**

4. RESULTS

In this section, the proposed WVD-based method is applied to several cases corresponding to healthy machine (Section 4.1) and machine with different levels of mixed eccentricity (Section 4.2). Finally, Section 4.3 studies the effect of non-fault-related phenomena on the diagnosis, through the analysis of signals corresponding to cases in which the eccentricity is combined with load torque fluctuations.

The motor considered for the simulations and experimental tests was a 35 kW motor with two parallel branches per stator phase. Detailed rated data of this motor are shown in Appendix B. The supply voltage and frequency were 200 V and 50 Hz, respectively. The sampling frequency f_s for capturing the signals was 16.6 kHz. The length of the register was 2.4 seconds. In all the tests, the current through one of the branches of the stator phase was analyzed (branch current).

Simulation signals were obtained by using a numerical FEM-based model of the 35 kW motor. The model enables the simulation of a wide range of faults. A full description of the model is given in [31]. A detailed description about fault implementation can be found in [32].

On the other hand, experimental tests were developed in the laboratory, loading the tested induction motor with a DC generator. The generator was connected to a resistor and its load controlled by changing the magnetizing current. Several startups were carried out, capturing the current signal through a Hall sensor current probe connected to a transient recorder, which enabled the storage of the

data for further analysis. The motor parameters were also monitored using a Power analyser. Figure 5 depicts a picture of the experimental test-bed.

4.1. Healthy machine.

Figure 6 shows the application of the WVD to the startup current of the unloaded healthy machine, after filtering the signal for elimination of the fundamental component and other Rotor Slot Harmonics not relevant for our analyses. Note the absence of any significant fault-related component in the time-frequency plane. Thus, a simple analysis of the spectra leads to confirm the healthy condition of the machine.

4.2. Machine with mixed eccentricity.

Several simulations, corresponding to different levels of eccentricity in the machine, were developed by using the FE-based model previously commented. WVD was applied to the resulting startup signals. Figures 7 and 8 show the time-frequency plane resulting from applying the WVD to the startup current signals corresponding to the machine with 20% mixed eccentricity in unloaded and loaded condition, respectively. The differences with respect the healthy case are clear.

First of all, the two most relevant eccentricity-related components clearly appear during the transient (EC-25 and EC-75, see Section 2). These two components show the aforementioned characteristic evolution during the transient; EC-25 decreases its frequency from 50 Hz (when the machine is connected, s=1) to around 25 Hz (=f-f_r) (s≈0), whereas EC-75 increases from 50 Hz (s=1) to 75 Hz (=f+f_r) (s≈0). As observed, these two components appear both for the unloaded and for the loaded machine; they can be used a reliable indicator of the presence of the fault.

But, in addition, the evolutions of other additional high-order eccentricity-related components can be also traced in these Figures. For instance, high-order components EC-100 and EC-125 appear in the

case of the machine in unloaded condition (Figure 7). Their respective evolutions towards 100 Hz (=f+2•f_r) and towards 125 Hz (=f+3•f_r) can be observed in that figure. In the case of the loaded machine (Figure 8), apart from the aforementioned high-order components (EC-100 and EC-125), it is even possible to detect other components, such as EC-150, which evolves towards 150 Hz (=f+4•f_r) and EC-175 which travels to 175 Hz (=f+5•f_r).

All these high-order components, as commented before, constitute additional sources of information for the diagnosis of the fault, complementing the information provided by the low order ones.

Experimental mixed eccentricity was forced in the laboratory. The eccentricity (predominantly dynamic) was obtained by assembling an eccentric spacer between the shaft and the inner rings of the bearings, as shown in Fig. 9. A measured value of 37% eccentricity was achieved [6].

Figure 10 shows the WVD of the startup current for this case. Evolutions of eccentricity-related components EC-25 and EC-75 are clearly observed. Also, components EC-100, EC-125 and even some traces of EC-150 and EC-175 are detected. This ratifies the validity of both the low and high order components for enabling the diagnosis the fault.

4.3. Machine with mixed eccentricity and load torque oscillations.

In this section, WVD of a startup current corresponding to the machine with eccentricity and operating under a certain fluctuating load torque is presented. This is a situation which can be rather common in certain applications in which machines with a certain level of eccentricity operate driving mills, compressors or other mechanisms introducing load torque oscillations. This case is quite usual in power generation plants [5].

Presence of load torque oscillations (as it happens with other phenomena such as supply voltage fluctuations) might introduce components quite similar to those associated with mixed eccentricities. Let us suppose, for instance, an oscillating load toque with constant modulating frequency of 25 Hz.

WVD of the startup current in this case would reveal two components, very similar to eccentricity-ones (EC-25 and EC-75), but not related to the fault. This can be seen in Figure 11 which shows the case of the healthy motor operating under the mentioned 25 Hz oscillating load torque. Two components at 25 Hz and 75 Hz appear. As commented, they could be confused with the eccentricity-related, leading to an incorrect diagnosis of the fault. Note, however, the absence of high-order harmonics in the time-frequency plane. A simple comparison between Figure 11 and Figure 7 or Figure 8 enables discarding the presence of the fault in the case of Figure 11, since the high-order eccentricity-related components are absent in that situation. Therefore, this case proves that the high-order eccentricity-related harmonics can constitute a complementary source of information in cases in which the low-order ones are not conclusive.

Figure 12 shows a case in which the mixed eccentricity fault coexists with a low torque oscillation with the characteristics commented before. The figure is quite illustrative; low-order eccentricity-related components appear (EC-25 and EC-75) but, as observed in the previous case, could be provoked by phenomena not related to the fault (indeed, in this case, they are amplified due to the load oscillation modulated at the same frequency). However, a detailed analysis of the time-frequency plane reveals the evolution of high-order components, such as EC-100, EC-125, EC-150 or EC-175. The presence of these components indicates the existence of the fault and, therefore, they constitute a crucial indicator for diagnosing the eccentricity in the machine.

6. A COMPARISON BETWEEN WVD AND DWT

The operation of the DWT was well described in previous works such as [4-5]. Without going into any further details, the DWT is a time-frequency decomposition tool that decomposes the analysed signal (in our case, the startup current) onto a set of signals named *wavelet signals* (one *approximation signal* and several *detail signals*). Each one of these wavelet signals is associated with a certain frequency band whose limits depend on the sampling frequency (f_s) of the signal being analysed and on the level of that wavelet signal [4]. Each wavelet signal extracts the time evolution of all the frequency components, contained in the analysed signal, belonging to the frequency band associated with that wavelet signal. In other words, the DWT performs a dyadic band-pass filtering of the signal being analysed [4-5].

The DWT has been used with success in the transient-based fault diagnosis field; the characteristic patterns appearing in the wavelet signals resulting from the analysis, caused by the transient evolution of fault-related components, have revealed as reliable indicators of the presence of the corresponding fault [4-5, 9, 14-15]. Nonetheless, the application of this tool for fault diagnosis purposes has been circumscribed to track the evolution of low frequency fault-related harmonics. Transient evolution of high-frequency fault-related components (and, more specifically, eccentricity-related) have been seldom investigated. Indeed, this has been mainly due to the dyadic filtering inherent to this transform and to the fact that, according to the Heisenberg principle, the higher the frequency resolution of a wavelet signal, the lower its frequency resolution is [33]. Actually, the high-order fault-related harmonics usually evolve (at least during most of their transient evolution) through the high-frequency region which is covered by the wavelet signals with lowest frequency resolution. This implies that the transient evolution of high-order fault-related components is mostly reflected by wavelet signals covering a very wide frequency range; therefore, these signals often contain different fault and non-fault related components, thus making often difficult the individual identification of a particular fault

component. Use of alternative tools such as Wavelet Packets (WP) or Continuous Wavelet Transforms (CWT) can overcome this drawback, but at the expense of increasing the time computational requirements.

The aim of this section is to provide a comparison between the WVD, proposed in this paper, and the DWT, applied in previous contributions but for the extraction of low-frequency eccentricity-related harmonics (mainly EC-25 and EC-75 in a machine with p=2, which were characterised in Table I). With this objective in mind, the DWT is applied here to the startup current signals of the 35 kW machine, considering 8 decomposition levels and using db-44 as mother wavelet, due to the better frequency response of this wavelet [15]. Since the sampling frequency for capturing the signals was f_s=16666 Hz, the frequency bands associated with the wavelet signals of interest for our analyses are those indicated in Table II [4-5].

Table II. Frequency bands associated with wavelet signals.

Signal	**Frequency band**
a_8	0 – 32.55 Hz
d_8	32.55 – 65.1 Hz
d_7	65.1-130.2 Hz
d_6	130.2-260.4 Hz

Figures 13 and 14 show the 8-level DWT decompositions of the startup currents for the healthy machine and for the machine with 20% eccentricity, respectively. The differences between both figures are immediately noticeable, mainly with regards to the wavelet signals a_8, d_7 and d_6. These differences are due to the evolution of the eccentricity-related components during the startup; for instance, the progressive increase in the amplitude of a_8 in Figure 14 is due to the transient evolution of eccentricity component EC-25, which starts evolving within signal d_8 at the beginning of the startup and it progressively penetrates within a_8, while its frequency decreases towards 25 Hz [4-5]. In Figure 13, since the machine is healthy, EC-25 has negligible amplitude and, hence, a_8 remains low. On the other hand, the progressive increment in amplitude of signal d_7 in Figure 14 is not totally but mostly caused

by the evolution of EC-75, as this eccentricity-related harmonic progressively penetrates within d_7 during its evolution from 50 Hz to 75 Hz during the transient. These evolutions were well characterised in [4-5], in which the eccentricity was diagnosed taking as a basis the evolutions of these two low-frequency components.

If the attention is now focused on the identification of the high-order fault-related components, it is also possible to track them in the wavelet signals resulting from the analysis. Indeed, EC-100 and EC-125 are also contributing to the gradual amplitude increment of wavelet signal d_7, as they progressively penetrate within the frequency band covered by this signal, during their frequency trip during the transient. Note that d_7 was already amplified by component EC-75. Here, the most important drawback of the DWT, already commented, for tracking high-order harmonics is revealed; since d_7 covers a wide frequency range (low frequency resolution), several fault components are contained within the same signal, thus becoming much worse their individual identification than with the WVD. On the other hand, EC-150 and EC-175 are the responsible for the amplitude increase of wavelet signal d_6, since this signal covers the frequency range containing the frequencies at which these components end their transient evolution. The same problem arises here; since d_6 is covering a wide frequency band (wider than d_7), this signal reflects the evolution of several fault-related components, which makes its individual tracking not possible.

This drawback of the DWT for tracking high-order harmonics can worsen if non-fault related components are present in the bands covered by these wavelet signals (a fact quite probable due to the possible presence of noises, load oscillations or other phenomena). In this case, the presence of these phenomena could make even more difficult the tracking of these harmonics, even leading to a possible incorrect diagnosis of the fault.

To sum up, although the DWT has revealed as an excellent tool for transient-based eccentricity diagnosis based on tracking the low-order components, it is desirable the use of other tools when

tracking the high-order harmonics; the WVD proposed in this contribution is just an option, which is proven here to be suitable for this objective, since it shows an excellent trade-off between frequency resolution at high and low frequencies. However, other currently developed techniques, based on tools such as CWT [34] or WP, also constitute interesting alternatives for achieving the same objective.

7. CONCLUSIONS

This work proves the usefulness of tracing the transient evolution of the high-order eccentricity-related harmonics as a complementary source of information for diagnosing the presence of this fault. Despite the fact that the study of the transient evolution of the low-order components (EC-25 and EC-75 for a machine with p=2) is often enough for diagnosing the eccentricity fault, in some situations (fluctuating load torques, supply voltage oscillations) the study of the frequency range through which these low-order components should evolve may not be enough for reaching a correct diagnosis conclusion, since similar components could be introduced by the aforementioned non-fault-related phenomena. Is in this context in which the study of the high-order components becomes relevant; the detection of their characteristic evolution enables to ratify the presence of the fault or, otherwise, to discard its existence. The present paper has proven this fact, through several simulation and experimental tests in which different healthy and faulty cases have been analysed, including situations in which eccentricity is combined with these other phenomena making difficult the diagnosis.

The paper proposes the use of the WVD for the time-frequency decomposition of the startup current signals, since this is a tool showing a good trade-off between time and frequency resolution both for low and high frequency region. A comparison with the DWT, which was successfully applied in the

past for tracking the low frequency eccentricity-related components, is carried out in the work; the comparison reveals the drawbacks of the DWT when tracking high-order harmonics, due to the low frequency resolution of the corresponding wavelet signals.

It should be said that research is continuously advancing in the signal processing field and progresses in other TFD tools (CWT, WP could make them valid for the simultaneous detection of both high and low-frequency components with enough resolution. So, the conclusions reached here with the WVD could be perfectly extrapolated to the time-frequency maps resulting from the CWT, WP, HHT, etc….The aim of this paper is to emphasize the usefulness of simultaneously tracing the transient evolution of low and high-order harmonics rather than the particular TFD tool being used for their detection.

In conclusion, the paper ratifies again the validity of the transient analysis for fault diagnosis purposes. It should be remarked that, although analyses shown here are focused on the startup transient (which, from an industrial perspective, would require to stop the corresponding machine, making difficult the implementation of the methodology in on-line diagnosis systems), analogue conclusions could be reached for other transients such as plug ~~plugging~~ stopping [14] or sudden load variations, which are rather common in machines operating in the industrial environment, a fact that shows the potential of the transient-based methodology for being implemented in on-line condition monitoring devices .

ACKNOWLEDGMENT

This work was supported by the Spanish “Ministerio de Educación y Ciencia”, in the framework of the “Programa Nacional de proyectos de Investigación Fundamental”, project reference DPI2008-06583/DPI.

APPENDIX A

MATLAB code that implements a suitable stop band filter to remove the main current component:

```
[B,A] = cheby1(2,0.5,[0.017 0.023],'stop')
wave=filter(B,A,wave);
```

Being 2 the half-order of the filter, 0.5 the peak-to-peak ripple in decibels in the pass band, and 0.017-0.023 the lower and upper limits of the frequency to be removed, taking into account that 1 is the top frequency, that is, half the sampling rate.

APPENDIX B

Characteristics of the tested motor:

Rated Power	35 kW	**Rated frequency**	100 Hz
Voltage	400 V	**Rated current**	64 A
Connection	Star	**Num pole pairs**	2
Num stators slots	48	**Num rotor bars**	40
Number of turns per coil	11	**Number of turns in series per stator branch**	44

REFERENCES

[1] S. Nandi, H.A. Toliyat, “Condition monitoring and fault diagnosis of electrical motors- A review”, *IEEE Transactions on Energy Conversion*, Vol. 20, No. 4, December 2005, pp.719-729.

[2] W.T. Thomson, M. Fenger, “Current signature analysis to detect induction motor faults”, *IEEE Industry Applications Magazine*, July/August 2001, pp. 26-34.

[3] J. Faiz, B.M. Ebrahimi, B. Akin, H.A. Toliyat , "Finite-Element Transient Analysis of Induction Motors Under Mixed Eccentricity Fault," *IEEE Transactions on Magnetics*, Vol.44, No.1, pp.66-74, Jan. 2008

[4] J. Antonino-Daviu, P. Jover, M. Riera-Guasp, J. Roger-Folch and A. Arkkio, "DWT Analysis of Numerical and Experimental Data for the Diagnosis of Dynamic Eccentricities in Induction Motors", *Mechanical Systems and Signal Processing, Elsevier,* Vol. 21, No. 6, August 2007, pp. 2575-2589.

[5] J. Antonino-Daviu, P. Jover Rodriguez, M. Riera-Guasp, M. Pineda-Sánchez, A. Arkkio, "Detection of Combined Faults in Induction Machines with Stator Parallel Branches through the DWT of the startup current" *Mechanical Systems and Signal Processing*, Elsevier, Volume 23, Issue 7, October 2009, Pages 2336-2351.

[6] M. Fernández Cabanas, M. García Melero, G. Alonso Orcajo, J.M. Cano Rodríguez, J. Solares Sariego. *Maintenance and diagnosis techniques for rotating electric machinery*. Marcombo-Boixareu Editores and ABB Service S.A, Barcelona, 1999.

[7] S. Nandi, S. Ahmed and H. Toliyat, "Detection of Rotor Slot and Other Eccentricity-Related Harmonics in a Three-Phase Induction Motor with Different Rotor Cages", *IEEE Transactions on Energy Conversion*, Vol. 16, No. 3, September 2001, pp. 253-260.

[8] R.R. Schoen, T.G. Habetler, "Evaluation and Implementation of a System to Eliminate Arbitrary Load Effects in Current-Based Monitoring of Induction Machines", *IEEE Transactions on Industry Applications*, Vol. 33, No. 6, November/December 1997, pp. 1571-1577.

[9] J. Antonino-Daviu M. Riera-Guasp, J. Roger-Folch and M.P. Molina, "Validation of a New Method for the Diagnosis of Rotor bar Failures via Wavelet Transformation in Industrial Induction Machines," *IEEE Transactions on Industry Applications.*, Vol. 42, No. 4, pp. 990-996, July/August 2006.

[10] H. Douglas, P. Pillay, and A. Ziarani , "Broken rotor bar detection in induction machines with transient operating speeds," *IEEE Transactions on Energy Conversion*, vol. 20, no. 1, pp. 135-141, March 2005.

[11] Z. Zhang and Z. Ren, “A novel detection method of motor broken rotor bars based on wavelet ridge,” *IEEE Transactions on Energy Conversion*, Vol. 18, No. 3 September 2003, pp. 417-423

[12] J. Cusido, L. Romeral, J. A. Ortega, J. A. Rosero, and A. Garcia Espinosa, "Fault Detection in Induction Machines Using Power Spectral Density in Wavelet Decomposition," *IEEE Transactions on Industrial Electronics*, vol. 55, pp. 633-643, 2008.

[13] A.Ordaz-Moreno, R.Romero-Troncoso, J.A.Vite-frías, J.Riviera- Gillen, A.García-Pérez, “Automatic online diagnostic algorithm for broken-bar detection on induction motors based on Discrete Wavelet Transform for FPGA implementation”, *IEEE Transactions on Industrial Electronics*, Vol.55, No.5, pp.2193-2200, May 2008.

[14] M. Riera-Guasp, J. A. Antonino-Daviu, M. Pineda-Sanchez, R. Puche, and J. Perez-Cruz, "A General Approach for the Transient Detection of Slip-Dependent Fault Components Based on the Discrete Wavelet Transform," *IEEE Transactions on Industrial Electronics*, vol. 55, pp. 4167-4180, 2008.

[15] J. Antonino-Daviu, M. Riera-Guasp, J. Roger-Folch, F. Martínez-Giménez, A. Peris, “Application and Optimization of the Discrete Wavelet Transform for the Detection of Broken Rotor Bars in Induction Machines,” *Applied and Computational Harmonic Analysis*, Elsevier, Vol. 21, September 2006, pp. 268-279.

[16] J. Pons-Llinares; J.A. Antonino-Daviu; M. Riera-Guasp; M. Pineda- Sanchez and V. Climente-Alarcon, *“Induction motor fault diagnosis based on analytic wavelet transform via Frequency B-Splines”*, in IEEE International Symposium on Diagnostics for EMPED, Cargèse, France, Aug. 31 – Sept. 3, 2009.

[17] F. Gu, Y Shao, N. Hu, A. Naid, A.D. Ball, Electrical motor current signal analysis using a modified bispectrum for fault diagnosis of downstream mechanical equipment, *Mechanical Systems*

and Signal Processing, In Press, Accepted Manuscript, Available online 16 July 2010, ISSN 0888-3270, DOI: 10.1016/j.ymssp.2010.07.004.

[18] F. Briz, M. W. Degner, P. Garcia, and D. Bragado, "Broken Rotor Bar Detection in Line-Fed Induction Machines Using Complex Wavelet Analysis of Startup Transients," *IEEE Transactions on Industry Applications*, vol. 44, pp. 760-768, 2008.

[19] R. Supangat, N. Ertugrul, W. L. Soong, D. A. Gray, C. Hansen, and J. Grieger, "Detection of broken rotor bars in induction motor using starting-current analysis and effects of loading," *IEE Proceedings Electric Power Applications*, vol. 153, pp. 848-855, 2006.

[20] Tsoumas, I.P.; Georgoulas, G.; Mitronikas, E.D.; Safacas, A.N.; , "Asynchronous Machine Rotor Fault Diagnosis Technique Using Complex Wavelets," *IEEE Transactions on Energy Conversion* , vol.23, no.2, pp.444-459, June 2008

[21] X. Fan, M.J. Zuo, "Gearbox fault detection using Hilbert and wavelet packet transform," *Mechanical Systems and Signal Processing*, Volume 20, Issue 4, May 2006, Pages 966-982

[22] V.K. Rai and A.R. Mohanty, "Bearing Fault diagnosis using FFT of intrinsic mode functions in Hilbert-Huang transform", *Mechanical Systems and Signal Processing, Elsevier*, Vol. 21, No. 6, August 2007, pp. 2607-2615

[23] Z.K. Peng, P.W. Tse, F.L. Chu, "A Comparison Study of Improved Hilbert-Huang Transform and Wavelet Transform: Application to Fault Diagnosis for Rolling Bearing", *Mechanical Systems and Signal Processing*, Elsevier, Vol. 19, 2005, pp. 974-988.

[24] D. Yu, J. Cheng and Y. Yang, "Application of EMD method and Hilbert spectrum to the fault diagnosis of roller bearings", *Mechanical Systems and Signal Processing*, Elsevier, Vol. 19, 2005, pp. 258-270.

[25] Puche-Panadero, R.; Pineda-Sanchez, M.; Riera-Guasp, M.; Roger-Folch, J.; Antonino-Daviu, J.A.; Perez-Cruz, J.; "Diagnosis of rotor bar breakages based on the Hilbert Transform of the

current during the startup transient" *Electric Machines and Drives Conference*, 2009. IEMDC '09. IEEE International . Publication Year: 2009 , Page(s): 1434 - 1440

[26] M. H. Benbouzid, "A review of induction motors signature analysis as a medium for faults detection" *IEEE Transactions on Industrial Electronics*, Vol. 47, No. 5, October 2000.

[27] L. Cohen, *Time-Frequency Analysis*. A.V. Oppenheim, Ed. Prentice Hall Signal Processing Series, New Jersey, 1995.

[28] J. Rosero, J. Cusido, A. Garcia, L. Romeral, J.A. Ortega, "Detection of Stator Short Circuits in PMSM by mean of joint Time-Frequency Analysis". IEEE International Symposium on Diagnostics for Electric Machines, Power Electronics and Drives, 2007. SDEMPED 2007

[29] M. Pineda-Sanchez, M. Riera-Guasp, J.A. Antonino-Daviu, J. Roger-Folch, J. Perez-Cruz, R. Puche-Panadero, "Instantaneous Frequency of the Left Sideband Harmonic During the Start-Up Transient: A New Method for Diagnosis of Broken Bars" *IEEE Transactions on Industrial Electronics*, Vol. 56, no.11, pp.4557-4570, November 2009.

[30] N. Wonchul and P. J. Loughlin, "When is instantaneous frequency the average frequency at each time?," *IEEE Signal Processing Letters*, vol. 6, pp. 78-80, 1999.

[31] Arkkio A., "Analysis of induction motor based on numerical solution of the magnetic field and circuits equations", *Acta Polytechn. Scand. Electri. Eng*. Serie 1987, On. 59, pp. 97, available at <http://lib.hut.fi/Diss/list.html#1980>.

[32] Pöyhönen S., Negrea M., Jover P., Arkkio A., Hyötyniemi H., "Numerical Magnetic Field Analysis and Signal Processing for Fault Diagnostic of Electrical Machines", COMPEL, *The international Journal for Computation and Mathematics in Electrical Engineering*, pp. 969-981, Vol. 22, No. 4, 2003.

[33] C.S. Burrus, R.A. Gopinath and H. Guo, Introduction to Wavelets and Wavelet Transforms. A primer, Prentice Hall, 1998.

[34] J. Pons-Llinares; J.A. Antonino-Daviu; M. Riera-Guasp; M. Pineda- Sanchez and V. Climente-Alarcon, “Induction motor fault diagnosis based on analytic wavelet transform via Frequency B-Splines”, in IEEE International Symposium on Diagnostics for EMPED, Cargèse, France, Aug. 31 – Sept. 3, 2009.

List of figure captions

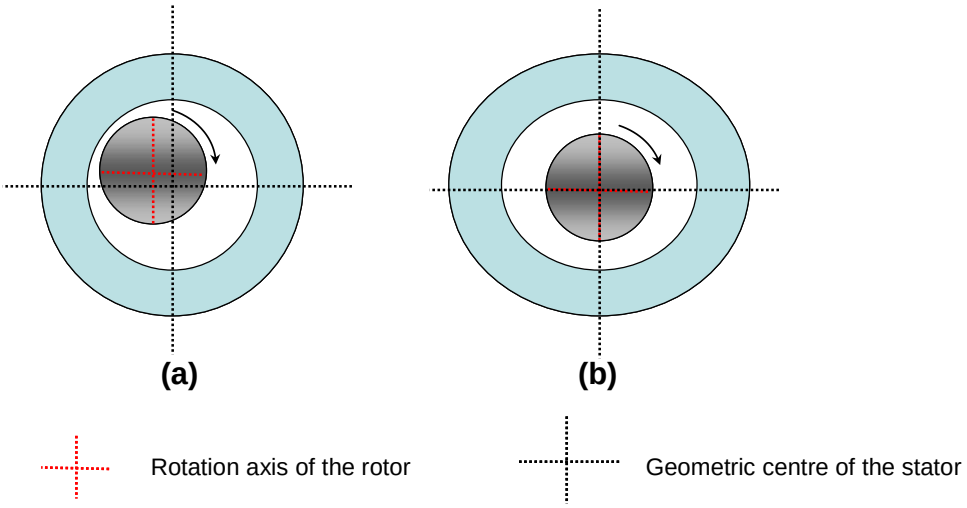

Figure 1. Cases of static eccentricity: (a) Incorrect placement of the rotor, (b) Ovality of the stator.

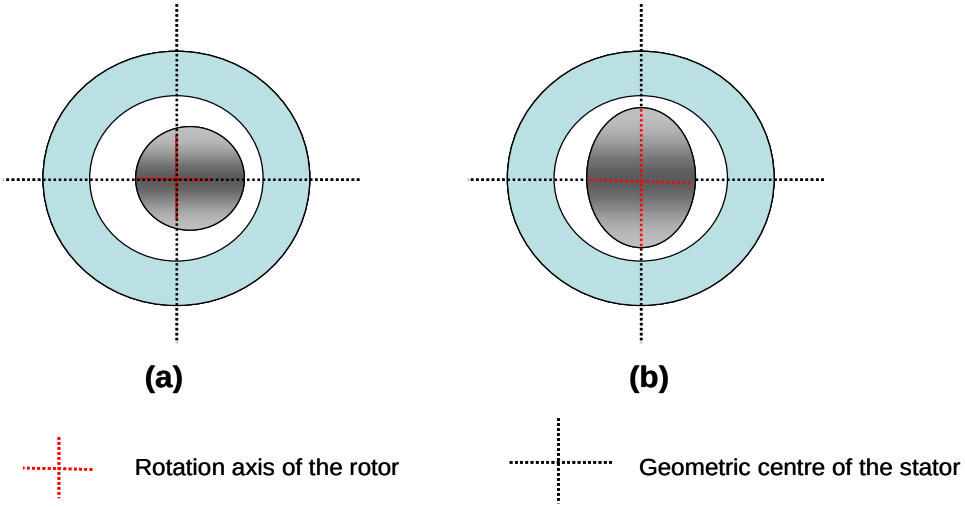

Figure 2. Types of dynamic eccentricity: (a) Non coincidence between rotation and geometric axes of rotor, (b) Ovality of rotor.

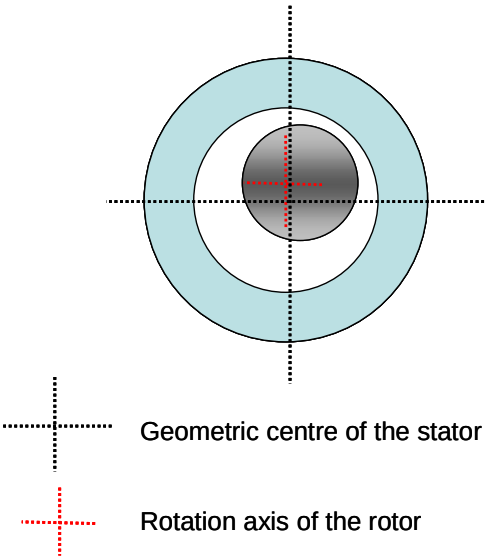

Figure 3. Case of mixed eccentricity.

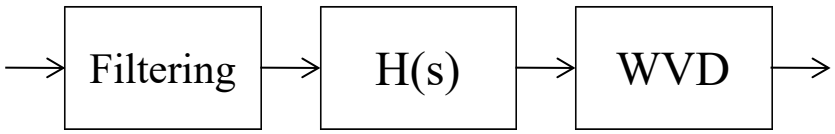

Figure 4. Proposed signal treatment approach.

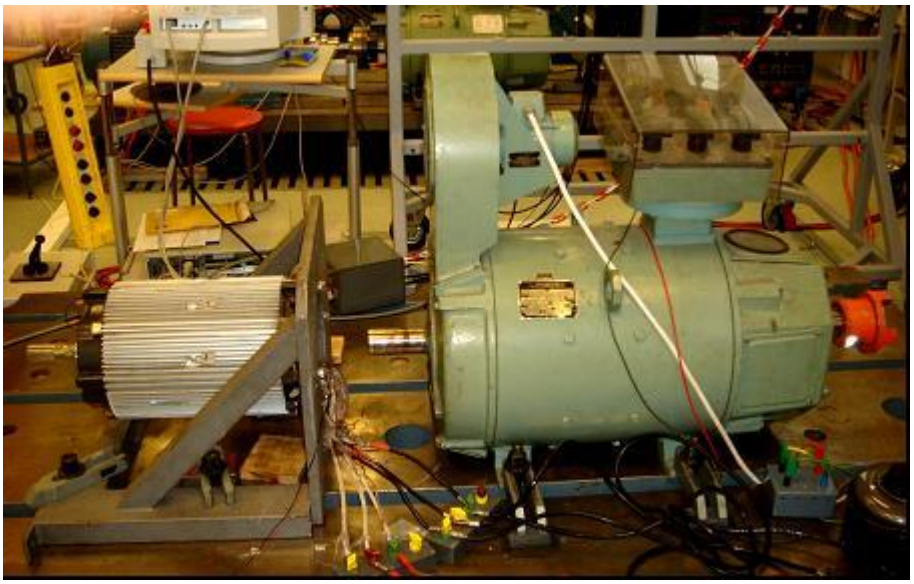

Figure 5. Experimental test-bed.

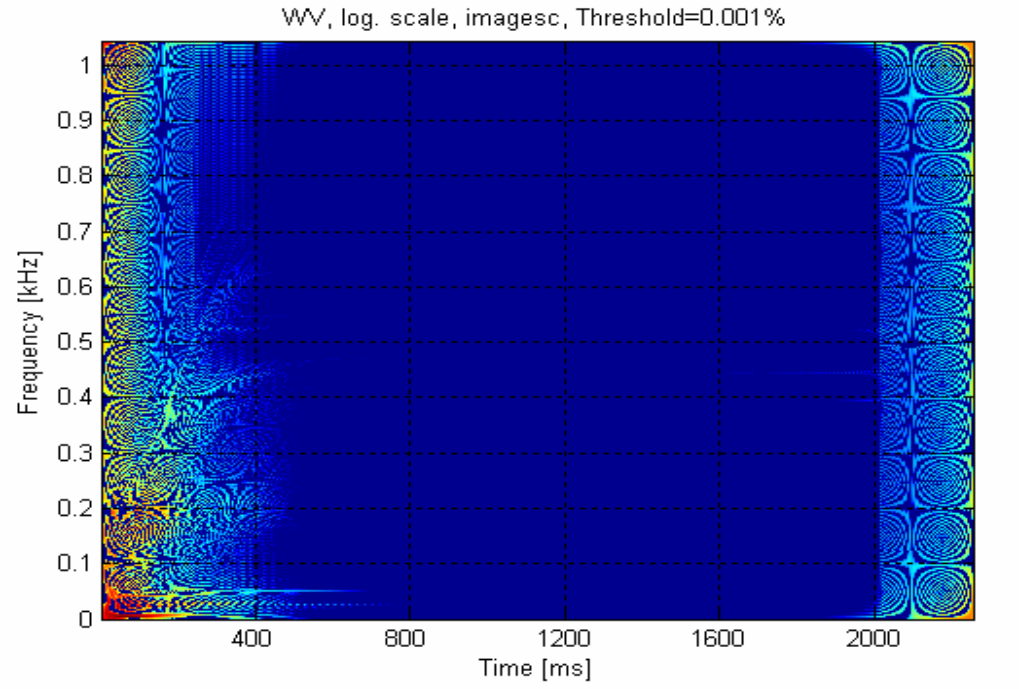

Figure 6. WVD of the startup current for the unloaded healthy machine (simulations).

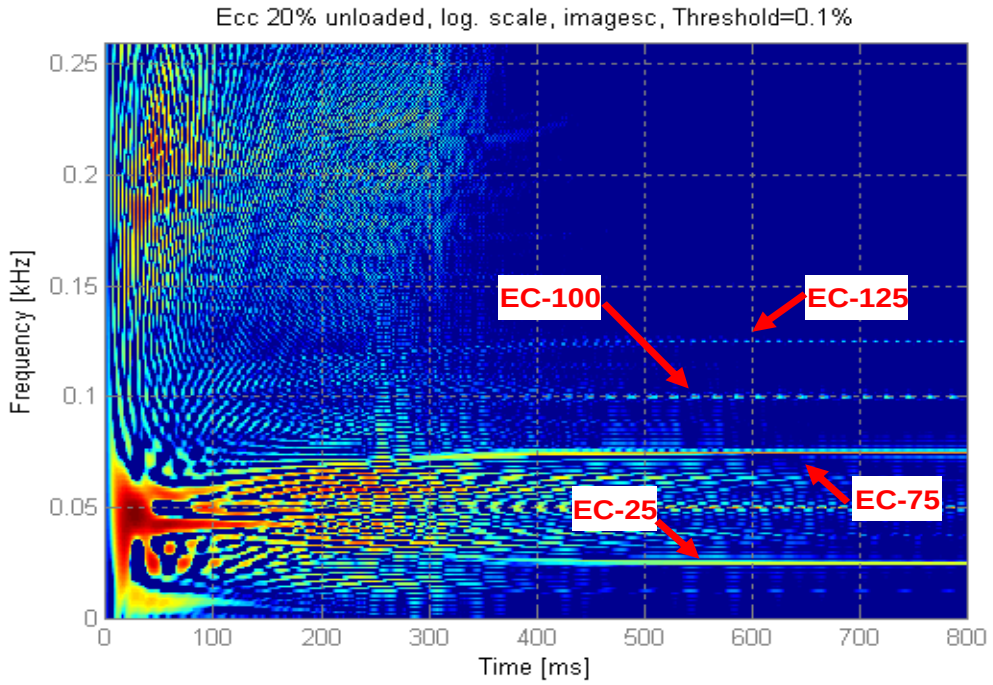

Figure 7. WVD of the startup current for the unloaded machine with 20% eccentricity (simulations).

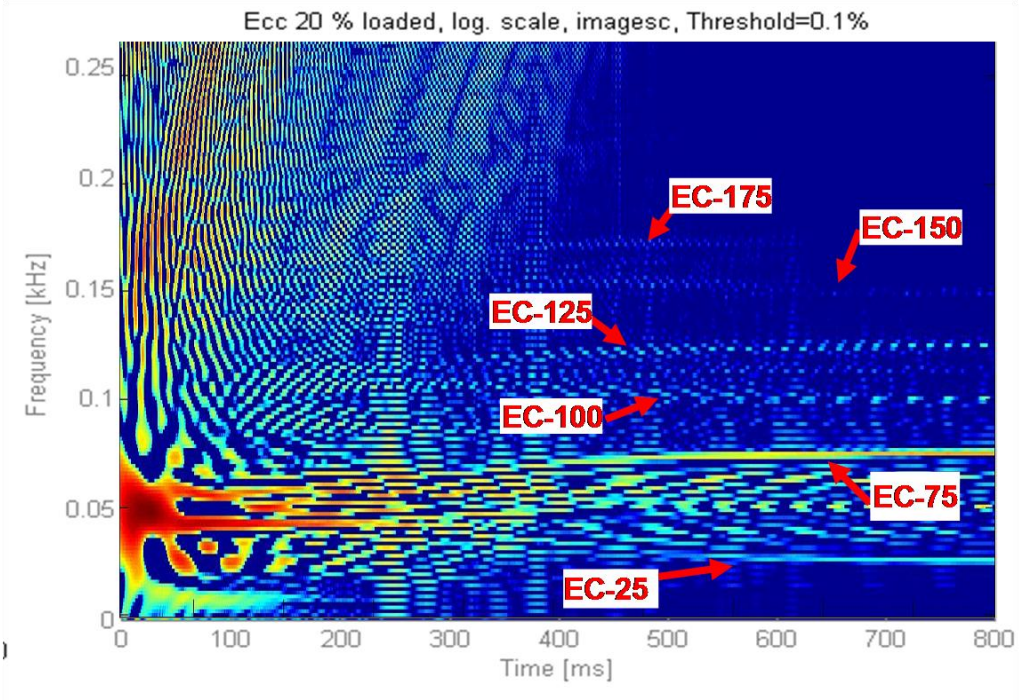

Figure 8. WVD of the startup current for the loaded machine with 20% eccentricity (simulations).

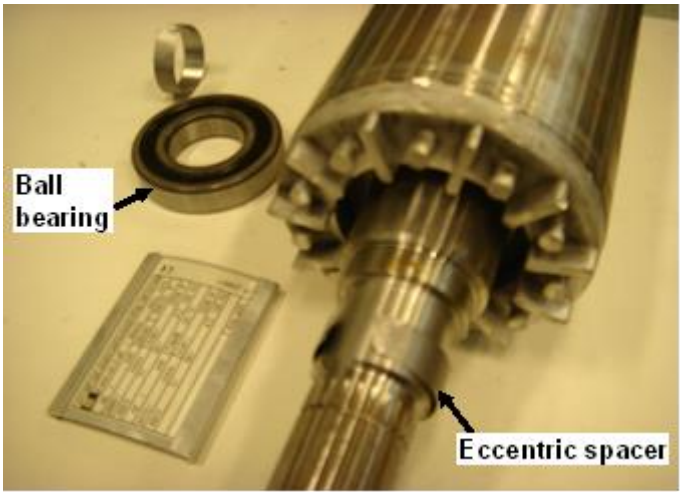

Figure 9. Elements for forcing the mixed eccentricity (predominantly dynamic).

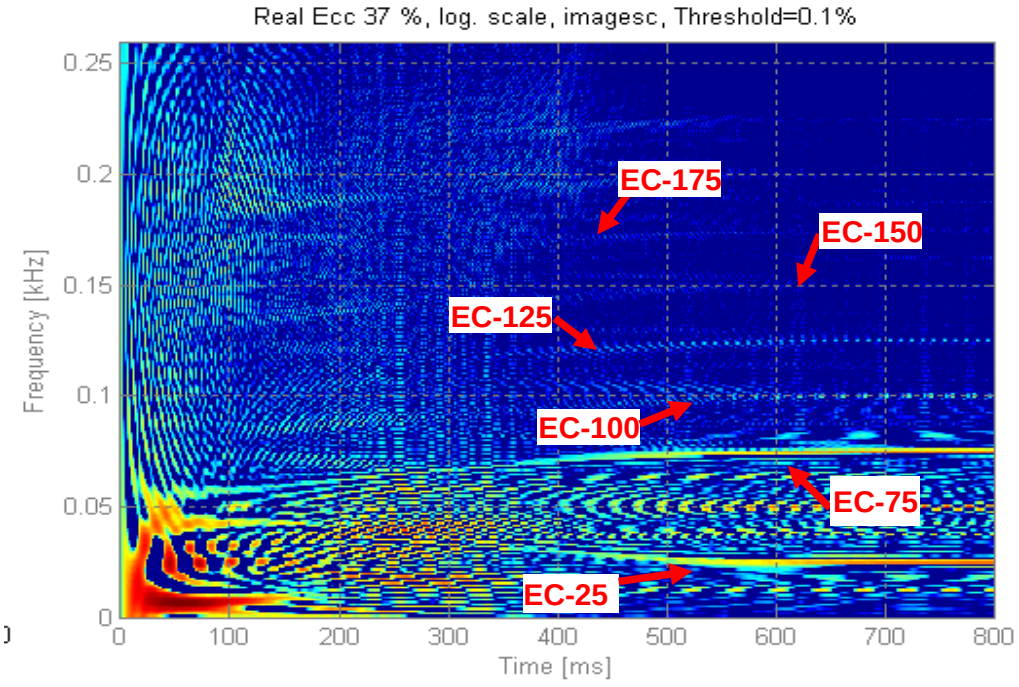

Figure 10. WVD of the startup current for the unloaded machine with 37% eccentricity (experiments).

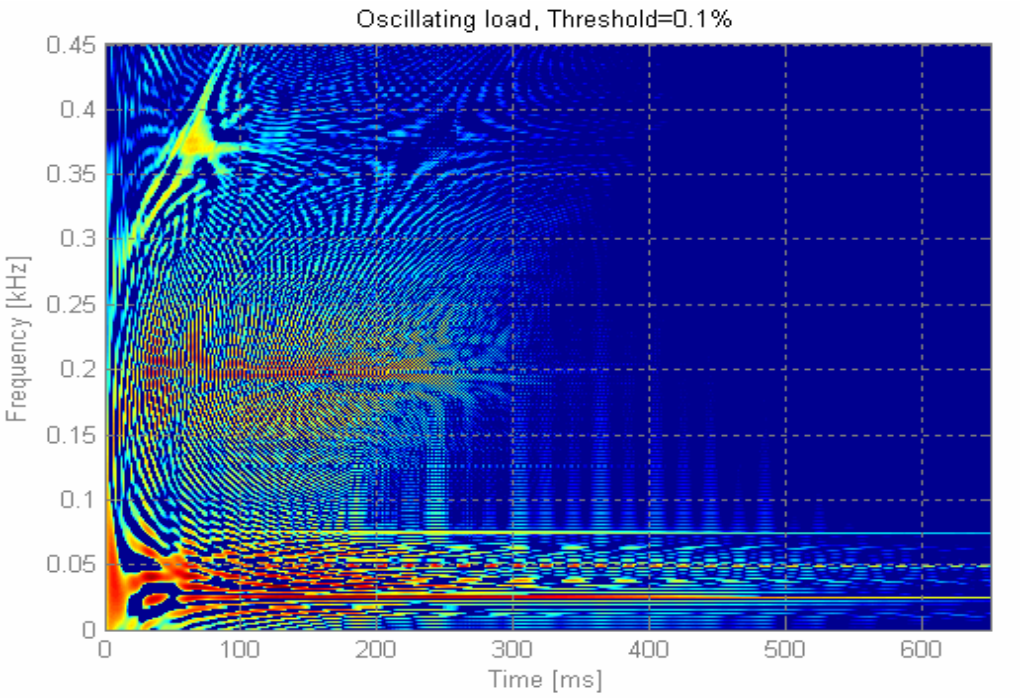

Figure 11. WVD of the startup current for the healthy machine with oscillating load (simulation).

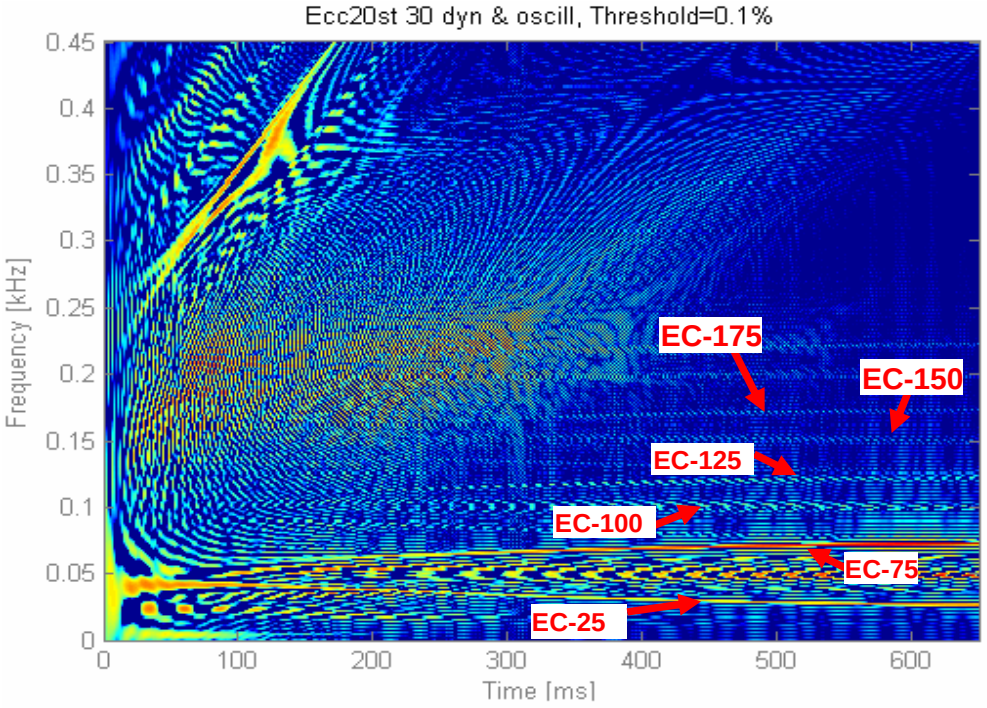

Figure 12. WVD of the startup current for the loaded machine with mixed eccentricity (20% static and 30% dynamic eccentricity) under oscillating load (simulation).

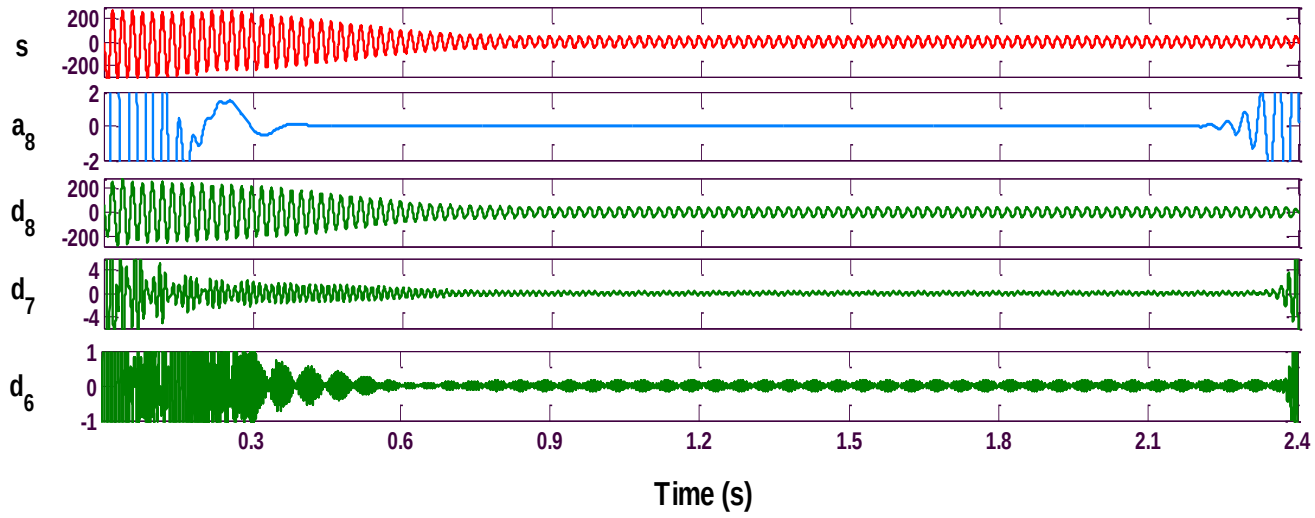

Figure 13. 8-level DWT analysis of the startup current for the healthy machine (simulation).

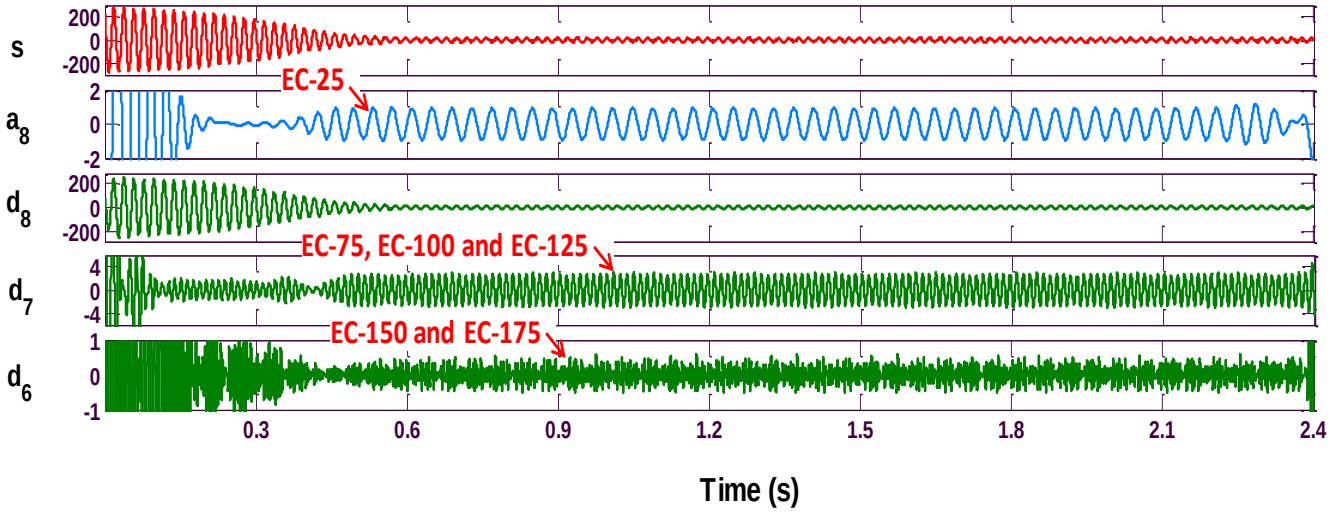

Figure 14. 8-level DWT analysis of the startup current for the machine with 20% eccentricity (simulation).